Biosensors and Bioelectronics 139 (2019) 111339

Contents lists available at ScienceDirect

Biosensors and Bioelectronics

journal homepage: www.elsevier.com/locate/bios

Power-free polydimethylsiloxane femtoliter-sized arrays for bead-based digital immunoassays

Jingjing Sun[a], Jiumei Hu[b], Tong Gou[a], Xiong Ding[b], Qi Song[a], Wenshuai Wu[b], Guoping Wang[b], Juxin Yin[a], Ying Mu[a,b,*]

[a] Research Centre for Analytical Instrumentation, Institute of Cyber-Systems and Control, State Key Laboratory of Industrial Control Technology, Zhejiang University, Hangzhou, Zhejiang Province, 310027, PR China
[b] College of Life Sciences, Zhejiang University, Hangzhou, Zhejiang Province, 310058, PR China

ARTICLE INFO

Keywords:
Paramagnetic beads
PDMS
Digital counting
Digital immunoassays

ABSTRACT

A novel microfluidic chip employing power-free polydimethylsiloxane (PDMS) femtoliter-sized arrays was developed for the detection of low concentrations of protein biomakers by isolating individual paramagnetic beads in single wells. Arrays of femtoliter-sized wells were fabricated with PDMS using well-developed molding techniques. Paramagnetic beads were functionalized with specific antibodies to capture the antigens. These antigens were labeled with enzymes via conventional multistep immunosandwich approach. After suspending in aqueous solutions of enzyme substrate, the solutions were delivered to the arrays using a conventional micropipette. The aqueous solutions were introduced into the microwells by capillarity and the beads were loaded into microwells by gravity. A fluorocarbon oil was then flowed into the chip to remove excess beads from the surface of the array and meanwhile isolated the femtoliter-sized wells. All processes were achieved by conventional micropipette, without external pumping systems and valves. Finally, the arrays were imaged using standard fluorescence imaging after incubation 30 min for digital counting enzyme molecules. It was demonstrated that the chip platform possessed the performance of digital counting with a linear dynamic range from 1 aM to 1 fM for the detection of biotinylated β-galactosidase (BβG), achieving a limit of detection (LOD) of 930 zM. Using this chip, a digital immunoassay to detect Tumor Necrosis Factor α (TNF- α) was developed. Since the chip fabrication is low-cost and circumvents the surface modification, we expect it can become a new chip-based digital immunoassay platform for ultrasensitive diagnostic of biomarkers.

1. Introduction

Quantitative detection of small numbers of biomolecules at low concentrations is of great interest for health monitoring, biological applications, and the clinical diagnosis of disease (Dong and Ueda, 2017; Tekin and Gijs, 2013). Enzyme-linked immunosorbent assay (ELISA) is widely used for the detection of protein biomarkers, as it amplifies the signals by using enzymes conjugated with antibodies. The conventional ELISA has a limit of detection of about 10^{-12} M concentration of the target (Giljohann and Mirkin, 2009), which compromises on detecting the samples with biomarkers at low concentrations of 10^{-16} to 10^{-12} M (Anderson et al., 2004; Hanash et al., 2011). Rissin and coworkers have developed a method for the detection of single molecules of proteins (i.e., digital ELISA), in which each biomarker-enzyme complex was isolated into ultra-small reactor volumes (fL) (Rissin et al., 2010).

Digital counting technology was first used in polymerase chain reaction (PCR) for absolute nucleic acid quantification by counting single molecules (Vogelstein and Kinzler, 1999). Beads-based digital ELISA works by capturing protein biomarkers on microscopic beads, labeling the protein biomarkers with an enzyme, isolating the beads in an array of femtoliter-sized wells, and detecting bead-associated enzymatic activity using fluorescence imaging. Adding an excess of beads to the sample containing a low concentration of protein biomarkers results in a Poisson distributed capture of target molecules by beads (roughly 10:1 beads to molecule ratio), meaning that 99% of beads carry either one or zero enzyme (Walt, 2013). Since the fluorescent product of the enzyme-substrate reaction is confined to a small volume rather than being free to diffuse into a large volume, it is possible to detect a single biomarker-enzyme complex using a conventional fluorescence

* Corresponding author. Research Centre for Analytical Instrumentation, Institute of Cyber-Systems and Control, State Key Laboratory of Industrial Control Technology, Zhejiang University, Hangzhou, Zhejiang Province, 310027, PR China.
E-mail address: muying@zju.edu.cn (Y. Mu).

https://doi.org/10.1016/j.bios.2019.111339
Received 28 January 2019; Received in revised form 17 May 2019; Accepted 17 May 2019
Available online 20 May 2019
0956-5663/

microscope (Liebherr et al., 2015; Rondelez et al., 2005). Therefore, protein biomarker concentration can be quantified through counting the number of "on" wells that contain a bead and enzyme, or "off" wells that contain a bead without enzyme. For high throughput, simultaneous and parallel analyses of single biomarkers-enzyme complexes, a mass of femtoliter-sized droplets or microchambers are required.

Rissin and his coworkers (Rissin et al. 2010, 2011) first developed the single-molecules arrays (SiMoAs) for digital detection. They established a microwell array platform on an optical fiber bundle that was loaded with individual paramagnetic beads using centrifugal forces and then mechanically sealed against a silicone gasket. However, fabricating and assembling femtoliter-sized well arrays using optical fiber glass bundles is expensive, highly manual, and requires a number of precision tools for manufacturing and instrument interfacing. Kan et al., (2012) proposed a DVD-based manufacturing method of femotoliter-sized wells arrays using injection molding of a well characterized hydrophobic material, namely cyclic olefin polymer (COP). However, due to the high contact angle of the bead solution on COP (~90°), a pumping system was used to apply vacuum pressure to the exit of the channel to draw the liquid into the channel and above the array, and the molds used for fabricating arrays had a draft angle of ~7–10° to avoid a perfectly vertical well wall. This microwell array disc addressed the limitations of the fiber-optic microwell arrays, facilitating the establishment of a commercial Simoa platform (Schubert et al., 2016; Wilson et al., 2016; Wu et al., 2016).

Efficient seeding of beads and simultaneous retaining of femtoliter droplets also can be accomplished using hydrophilic-in-hydrophobic microwells that has a hydrophilic bottom and hydrophobic interwell surface. Kim et al., (2012) proposed a device employing one million hydrophilic-in-hydrophobic microwells by ion etching glass coated hydrophobic polymer of carbon-fluorine (CYTOP) which can be manipulated using a micropipette. Deborah Decrop et al., (2017) described a fabrication of arrays with hydrophilic-in-hydrophobic microwells using a novel single-step fabrication procedure by stamp molding of a hydrophobic OSTE-polymer formulation that does not require post-maufacturing surface modification. Leirs et al., (2016) described a digital microfluidic platform with 62,500 hydrophilic-in-hydrophobic femtoliter-sized microwells patterned in Teflon-AF layer deposited on glass slides (Witters et al., 2013) to detect influenza A nucleoprotein. Despite that the hydrophilic-in-hydrophobic nature allows effective embedding of individual beads with fluid droplets in each microwell, the manufacture of hydrophilic-in-hydrophobic chips is unfortunately often expensive or labor-intensive.

Another effective strategy for high-sensitivity detection using ELISA is to isolate each biomarker-enzyme complex into ultra-small droplets. Shim et al., (2013) reported a microfluidic droplet-based approach used to generate and manipulate 32 fL water-in-oil droplets at a frequency of 3.5×10^5 Hz. Using microfluidic droplets can overcome the limits on the scalability and flexibility of mechanical fabrication of femtoliter wells. However, a complex storage area is needed for trapping the femtodroplets that are packed into a monolayer in storage by monolithic microfluidic valves, so that the fluorescence measurements of individual droplets can be achieved by a fluorescence microscope.

These methods above offer several smart strategies to overcome the concentration limitation of conventional ELISA, here, we demonstrate a simpler power-free microfluidic chip suitable for the quantitative detection of extremely low concentrations of protein biomarkers with digital counting. We have generated large arrays of one million femtoliter-sized wells in PDMS by molding techniques. The beads suspension was introduced into the microwells by capillarity (Rondelez et al., 2005) and the beads were loaded into microwells by gravity. All processes were achieved by conventional micropipette, without external pumping systems and valves. A fluorocarbon oil was used to remove excess beads from the surface of the arrays, and to seal and isolate the femtoliter-sized wells (Zhang et al., 2012).The use of power-free femtoliter-sized PDMS arrays greatly simplifies the loading of beads and the isolation of single beads in femtoliter volumes. This chip is low-cost in manufacturing and do not need complex surface modification. Since one million wells allowed us to simultaneously examine roughly 6×10^5 beads for the presence of biomolecules, the LOD of this chip achieved 930 zM for the detection of BβG. Moreover, digital ELISA of TNF-α showed a LOD of ~50.48 fg/mL (2.88 fM).

2. Materials and methods

2.1. Materials

The negative photoresist (SU-8 2000, 3050) and developer were bought from MicroChem (Westborough, MA, USA). PDMS (RTV-615 A and B components) were purchased from Momentive Performance Materials (Waterford, NY, USA). Trimethylchlorosilane was obtained from Aladdin (Shanghai, China). Biotinylated β-galactosidase (BβG), fluorogenic substrate fluorescein di (β-D-galactopyranoside) (FDG), bovine serum albumin (BSA), Tween-20, $MgCl_2$, were purchased from Sigma Aldrich (St. Louis, MO, USA). Lodestar superparamagnetic beads with streptavidin functionalization and carboxyl functionalization were obtained from Agilent technology (Santa Clara, CA). Monoclonal anti-TNF-α antibody, recombinant TNF-α calibrator, and detection anti-TNF-α antibody were purchased from R&D System (Waltham, MA, USA). The streptavidin-β-galactosidase (SβG) was obtained from Life Technology (Grand Island, NY, USA). Starting Blocking T20 PBS (TPBS) was purchased from Thermo Scientific (Waltham, MA, USA). Bovine serum, 1-ethyl-3-(3-dimethylaminopropyl) carbodiimide hydrochloride (EDC) were purchased from Sangon Biotech (Shanghai, China). Fluorinated oil FC-40 was obtained from 3M (St. Paul, MN, USA).

2.2. Fabrication of silicon master and chip

The chip was composed of array layer, channel layer and glass layer that was fabricated using a well-developed soft lithography replica molding process. Fig. 1 shows the schematic of the fabrication process. In brief, the master molds with positive features were fabricated by patterning negative photoresist on silicon wafers using conventional photolithography techniques. A 120 μm layer of SU-8 3050 negative

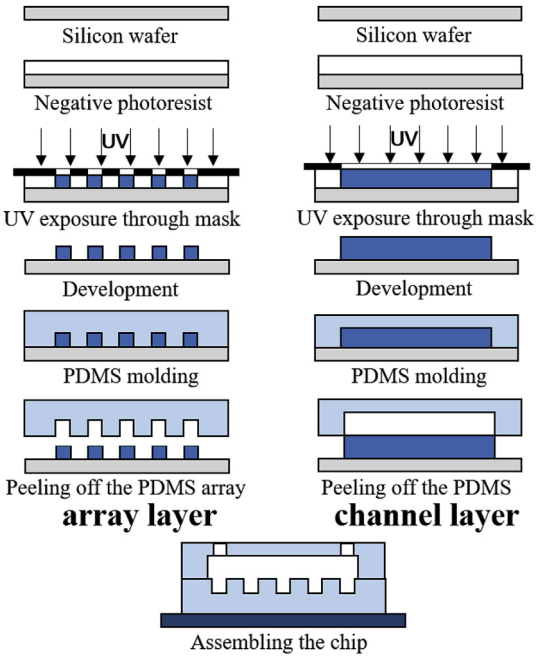

Fig. 1. Schematic of the fabrication process of power-free femtoliter-sized arrays.

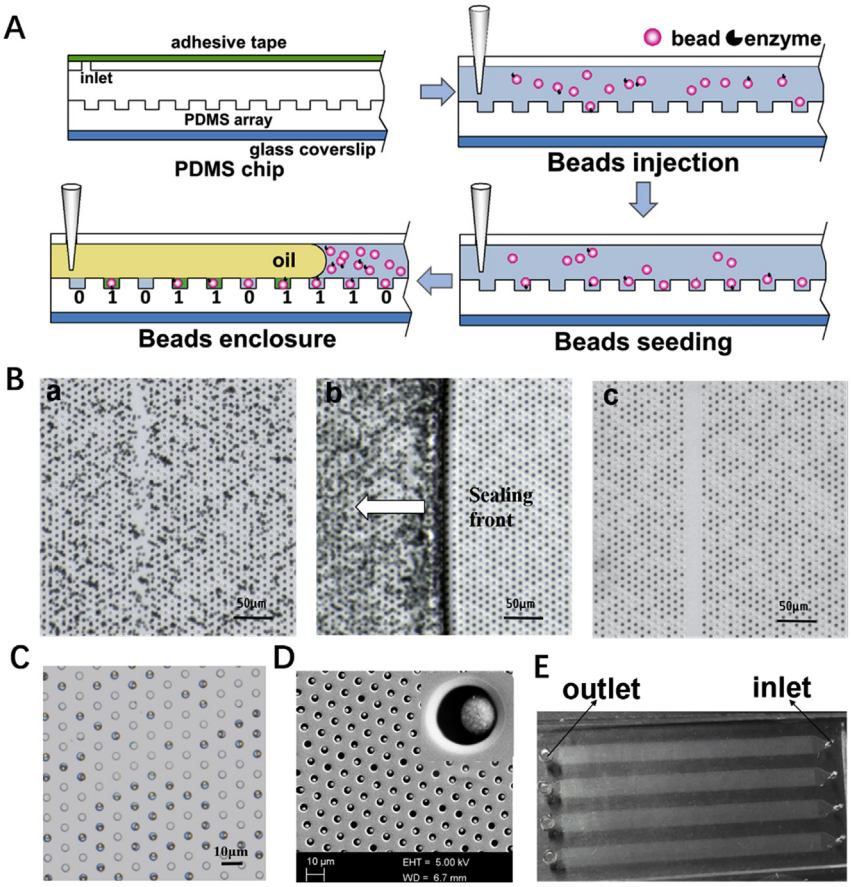

Fig. 2. Schematic illustrations of bead trapping and beads are trapped into the single wells. (A) Schematic illustrations of bead trapping. Aqueous solution with target beads is injected into the chip through inlet well by using a conventional micropipette. The injected beads are allowed to settle down because of gravity for several minutes. Then, oil is injected through the inlet and aqueous solution containing a single bead is sealed in the well. (B) Optical microscopy images show the process of sealing wells and removing excess beads. (a) The beads were loaded into the femtoliter-sized wells with excess, unloaded beads on the surface. (b) The aqueous/oil interface where the excess beads on the surface were being pushed towards the aqueous phase. (c) The excess beads were removed and the retaining beads were loaded into the femotoliter-sized wells. (C) Light-field images of the femtoliter arrays. Beads (2.7 μm in diameter) are trapped into the single wells (4.4 μm in diameter, 3.5 μm in deep, 10 μm center-to-center distance). (D) SEM images of array microwells showing the presence of singulated beads. (E) Fabricated chip. Each chip has 4 channels. There are 184 blocks of well array where each block has 5520 wells corresponding to the 10^6 microwells on a single channel.

photoresist was applied by spincoating for 30 s at 1000 rpm onto a clean silicon wafer followed by baking at 95 °C for 3 min and exposed to collimated UV light through a film mask that contained the channel pattern. And another clean silicon wafer was spincoated at 1000 rpm for 30 s to achieve a 3.0-μm thick layer of negative photoresist and exposed to collimated UV light (250 mJ/cm^2) through a chrome-on-glass mask that contained the array pattern. Wafers were developed in SU-8 developer at room temperature. Then the molds were baked onto a hot plate at 200 °C for 40 min.

The molds are silanized with trimethylchlorosilane in a fuming hood for 30 min at room temperature to prevent undesired bonding between PDMS and the molds. The PDMS pre-polymer is prepared by mixing a base and curing agent in a ratio of 5:1 and 10:1 (v/v). The 5:1 and 10:1 PDMS pre-polymers were poured over the channel layer mold and the array layer mold respectively and cured for 25 min on an 85 °C hot plate. The PDMS was then peeled off from the silicon masters and cut into appropriate pieces. Prior to bonding, inlet ports and outlets ports were created in the channel layer using a 1.0 mm Harris Micro-Punch. And then, the array layer put on one glass slide and pressed together to exclude the bubble between them. Next, the channel layer and the array layer were manually aligned and pressed together to promote bonding. The assembly of three layers were bonded together by baking at 85 °C overnight.

2.3. Digital counting of BβG

Superparamagnetic beads with streptavidin functionalization were mixed with various concentrations of BβG (400 μL) from 1 aM to 100 fM in a test tube. After reaction for 2 h at room temperature, the beads were washed three times in PBS with 0.1% Tween-20 and 0.1% BSA, and three times in PBS with 0.1% Tween-20. The beads were then resuspended in 15 μL of 250 μM FDG in PBS with 0.1% Tween-20 and 1 mM $MgCl_2$ and introduced into the arrays. The beads were settled for 2 min, and trapped into the droplet array by injecting fluorinated oil. The chip was incubated at room temperature for up to 30 min to increase the signal-to-noise ratio.

2.4. Digital ELISA of TNF-α

Carboxyl-terminated paramagnetic beads were functionalized with a monoclonal anti-TNF-α antibody to TNF-α using EDC coupling according to the manufacturer's instructions. Test solutions (100 μL) composed of TNF-α spiked into 25% bovine serum in TPBS were incubated with suspensions of 3×10^6 magnetic beads for 2 h at room temperature. The beads were then separated and washed three times in 5 × PBS and 0.1% Tween-20. The beads were resuspended and incubated with solution containing biotinylated polyclonal anti-TNF-α (1 nM) in TPBS for 1 h at room temperature. Next, the beads were then separated and washed three times in 5 × PBS and 0.1% Tween-20. The beads were then incubated with solutions containing SβG (40 pM) for 30 min at room temperature, separated and washed six times in 5 × PBS and 0.1% Tween-20 before injection into the chip and one time in PBS. The beads were then resuspended in 15 μL of 250 μM FDG in PBS with 0.1% Tween-20 and 1 mM $MgCl_2$ and introduced into the arrays. The beads were settled for 2 min, and trapped into the droplet array by injecting fluorinated oil. The chip was incubated at room temperature for 30 min and then acquired images.

2.5. Image acquisition and analysis

Bright-field and fluorescence images of one array block were acquired sequentially by using an inverted microscope (IX71, Olympus). The arrays were illuminated with white light and imaged on the CCD camera. After the white light images were acquired, fluorescence

images were acquired (495 nm excitation; 520 nm emission) with an exposure time of 2000 ms. Then the stage was manually moved to acquire images of the next block in an array. The bright-field and fluorescence images were analyzed using image J software. At first, the bright-field images and fluorescent images were converted into grey-scale images. By using the "Analyze Particles" module in the software, the number of fluorescent wells (F) and the number of wells containing bead (B) could be counted. Then the percentage of fluorescent microwells can be calculated through dividing F to B.

3. Results and discussion

3.1. Chip fabrication and performance of loading and sealing

As shown in Fig. 1, the configuration of power-free femtoliter PDMS arrays is comprised of three functional components arranged in sandwich format, the channel layer, array layer, and glass layer. The glass layer is used to prevent the deformation of PDMS layers during the experiments. The microwells are 4.36 ± 0.18 μm in diameter and 3.49 ± 0.17 μm in deep, giving a volume of approximately 50 fL, which are slightly bigger than the beads (2.7 μm in diameter) (see Fig. 2C). The whole channel allows to be injected ~15 μL of bead suspension. Fig. 2D shows the scanning electron microscopy (SEM) image of the array, illustrating the well uniformity and surface flatness. Thus, the femtoliter PDMS arrays yield structures with acceptable well geometries and dimensional uniformity.

The key to beads-based digital ELISA is to make sure that only one bead is trapped into the single wells. The loading process are shown in Fig. 2A. Aqueous solution with target beads is injected into the chip through inlet well by a conventional micropipette. The injected beads are allowed to settle rapidly inside the fluidic channel under the influence of gravity, because the beads contain 13.9% by weight of iron. Fig. 2C illustrates an outcome of the bead loading process and one well contains one single bead. Furthermore, bead loading in these chips is sensitive to bead concentration and the time allowed to settle. Figure S-1 shows bead loading efficiency as a function of bead concentration and time. Quantitative analyses of images showed that ~63% of wells were occupied by a bead after 2 min of bead settling via gravity using 3×10^6 beads in 15 μL.

After delivery of beads into the channels, not all of the beads fall into the wells. In other words, excess beads remained on the surface of the array. These beads could interfere potentially with sealing and also cause extraneous fluorescent signals, if not removed from the array area during the imaging. High-density oil allowed to efficient removal of the aqueous solution from the hydrophobic surface and retained the aqueous solution with trapped beads. In this process, we used the fluorocarbon oil FC 40 to displace the aqueous in the direction of flow, thereby washing away the excess beads on the surface (see Fig. 2B (a)). Fig. 2B (b) illustrates that there is a clean surface in the trailing side of the interface in the direction of flow. Also, this method resulted in complete removal of excess beads from the surface (see Fig. 2B (c)). The process only takes about 10 s to achieve the extremely high frequency of embedded droplets generation on single array.

Because PDMS is a hydrophobic material, to test the loading performance of chip, we introduce three different solutions into microwells. Solutions of calcein, fluorescein and FDG with beads incubated with high concentration of BβG (1pM) was injected into the arrays, and then isolated and sealed wells by FC40 and took fluorescent photos (see Fig. 3A). We found that not all kind of aqueous solutions can achieve a distribution by capillarity (Fig. 3A (a)). Due to the gas solubility of PDMS, air dissolved in PDMS can be evacuated by putting the PDMS chip in a vacuum pump for a certain period of time and the negative pressure is generated within the PDMS (Song et al., 2011; Zhu et al., 2012). Using this degassed chip, the sample solution can be introduced into the chip efficiently. In our experiment, we have made a comparison for the sampling effect using both undegassed and degassed chips. To the arrays of control group was put into a vacuum pump before using it. The three solutions were then loaded into the degassed chip under the actuation of the negative pressure, and were imaged under microscope afterwards. As shown in Fig. 3B (a), solution of calcein was introduced into the wells. Solutions of fluorescein and FDG with beads were also introduced into the wells and there were no distinctly difference in terms of the sampling effect between undegassed chip and degassed chip (Fig. 3B (b, c)). So, in this study, the chip did not need to be degassed and no any pumping systems were required. That is why we termed our method as "power-free".

3.2. Single-molecule detection of β-galactosidase

To test the single-molecules detection ability of the chip, BβG was detected by first capturing it with streptavidin-coated superparamagnetic beads. When the ratio of beads to enzymes is 10:1, 99% of beads carry either one or zero enzyme, according to the Poisson distribution, and thus protein concentration can be quantified by counting the number of "on" or "off" wells. A fixed number of beads (3×10^6) was incubated with different concentrations of BβG (1 aM–100 fM) in a fixed volume (400 μL), after which the beads were sealed in the chip with 250 μM FDG by injecting FC 40. A fluorescent image was taken right 30 min after the sealing. Sealing confines the fluorescent product generated from the reaction between an enzyme and substrate to inside individual femtoliter-sized wells, creating a locally high concentration of product (Figure S-2). The brightness of wells containing bead and enzyme (Fig. 4A (c)) are clearly different from the brightness of background (Fig. 4A (a)) and the brightness of wells that contain bead without enzyme (Fig. 4A (b)). The numerical ratio of wells containing bead and enzyme to wells containing bead yields the concentration of the target analyte. Thus, the larger the number of available wells in a measurement, the better the detection sensitivity that can be accomplished in a given assay time. Fig. 4B shows fluorescence images of the array and illustrated how the number of wells showing fluorescence increases as the concentration of BβG increases. Fig. 5A shows a log-log plot of the concentration of BβG as a function of the percentage of fluorescent wells. A linear trend in digital enzyme quantification was obtained for BβG concentrations between 1 aM and 1 fM (Fig. 5B, $R^2 = 0.996$). The LOD of BβG detection was determined from the extrapolation of BβG at a fraction of bright wells equal to the background plus three times standard deviation of the background. The background was determined from the experiments without BβG molecules. By this way, the LOD reached 930 zM, which was a little higher than the LOD of SiMoAs (220 zM).

3.3. Detection of TNF-α using power-free PDMS femtoliter-sized arrays

The power-free PDMS femtoliter-sized arrays were applied to the detection of the clinical biomarker TNF-α. The ability to sensitively detect BβG paves the way for ultrasensitive quantification of very low concentrations of TNF-α. In the first step of the bead-based digital ELISA, microscopic beads coated in antibodies capture the target protein, followed by labeling the bound proteins with enzyme reporter molecules. Enzyme labeling of the proteins is achieved by the formation of an immunocomplex in two steps, using a biotinylated detection antibody and a streptavidin-enzyme conjugate (Figure S–3A). The method is conceptually similar to the digital ELISA reported by Rissin et al., (2010). Beads associated with bound enzyme label and labels generate a locally high concentration of fluorescent product in the 50-fL reaction chambers (Figure S–3B). In digital ELISA, the number of bright wells in the fluorescence images was proportional to the concentration of TNF-α. Using digital ELISA to detect TNF-α in 25% bovine serum, we obtained an LOD of ~12.62 fg/mL (0.72 fM), which equates to an LOD in whole serum of ~50.48 fg/mL (2.88 fM). The LOD is determined by the background plus three times the standard deviations of the background, where the background was acquired without TNF-α molecules (Fig. 6).

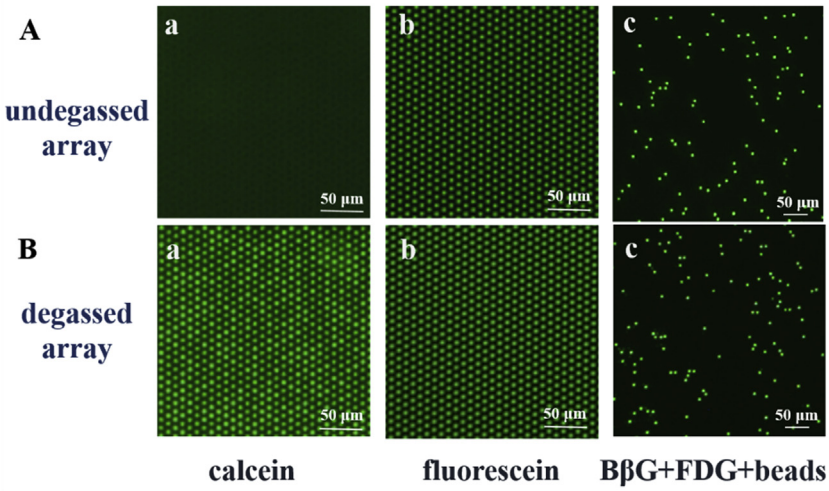

Fig. 3. Fluorescence image of undegassed and degassed arrays injected by the solutions of calcein, fluorescein and beads with FDG. Three solutions were injected into (A) undegassed and (B) degassed arrays, respectively. Then isolating and sealing the wells by FC40. (A) (a) Solution of calcein didn't get into the wells so the wells do not have the fluorescence. (b,c) Solutions of fluorescein and FDG with beads were introduced into the wells and the wells have the fluorescence. (B) Three solutions were all get into the wells and the wells have the fluorescence. Before the experiment, streptavidin-coated superparamagnetic beads incubated with 1 pM BβG.

The LOD of the chip was at the same order of magnitude of the LOD of the commercial platform Simoa HD-1 Analyzer (14 fg/mL) (Wilson et al., 2016).

4. Conclusions

In summary, a novel power-free microfluidic chip have been developed for high-sensitive detection of protein biomarkers. The obtained microwells arrays are shown to have appropriate geometries and dimensional uniformity. And successful generation of one million embedded droplets and seeding of individual paramagnetic in the microwell array were demonstrated. This bead-based approach enables the quantification of very low abundance biomarkers by integrating a bead-based immunoassay with direct digital counting of individual enzyme

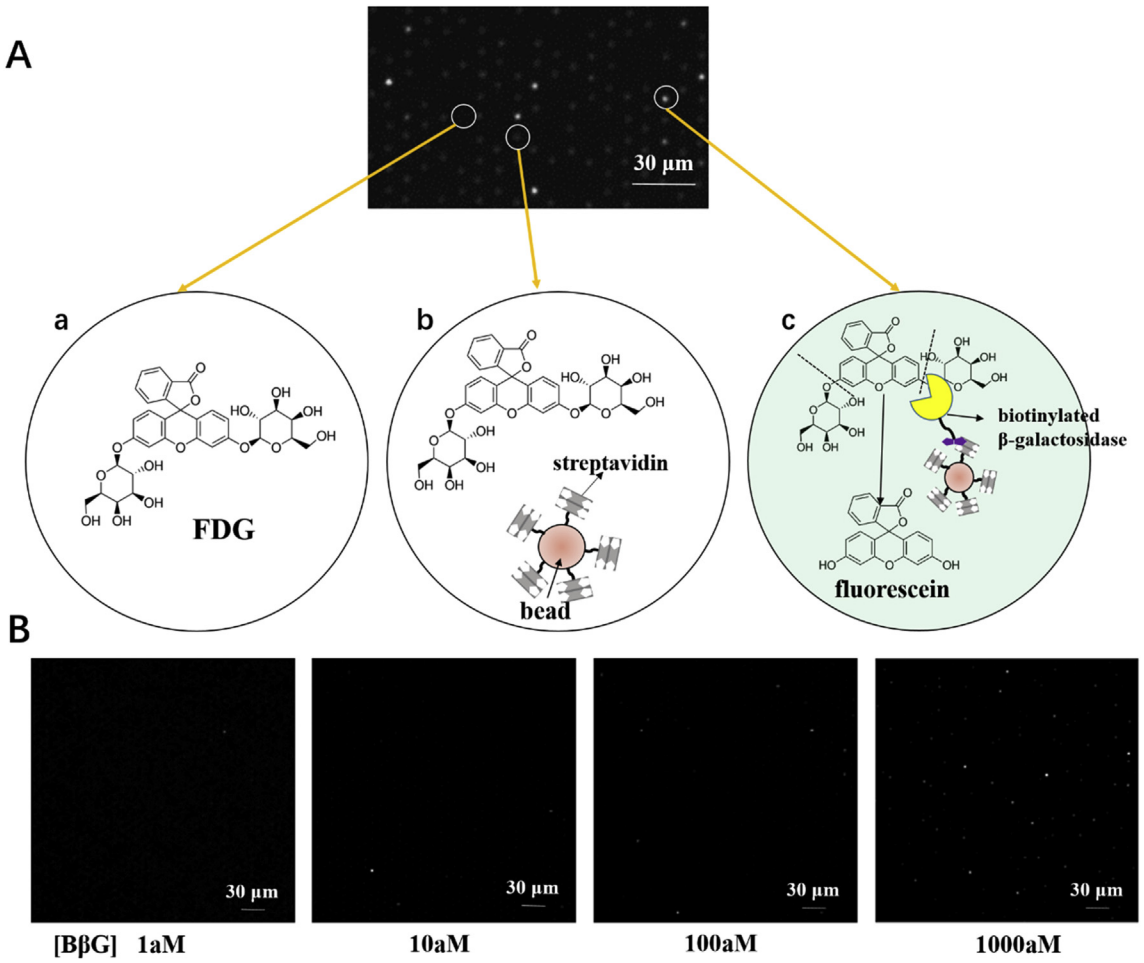

Fig. 4. Single-molecule detection of β-galactosidase. (A) Schematic of three populations of wells after incubation: (a) wells containing no bead, (b) those containing a bead without enzymes, and (c) those containing a bead with an enzyme exhibiting a positive signal due to the enzymatic activity of a single β-galactosidase reporter. (B) Fluorescence images of the array for various concentrations of BβG.

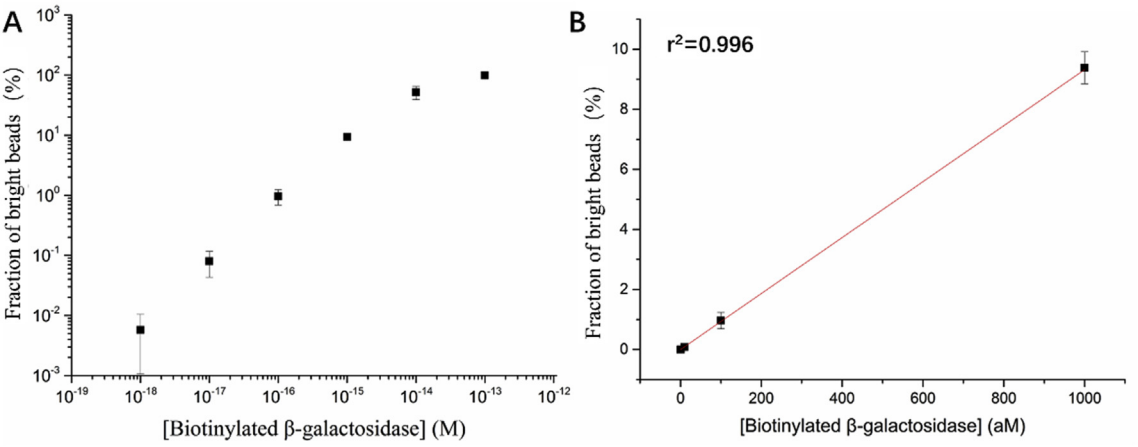

Fig. 5. Single-molecule detection of biotinylated β-galactosidase (BβG). (A) A log-log plot of the concentration of BβG as a function of the percentage of bright wells. (B) Expanded plot with linear-linear scale. The limit of detection (930 zM) was determined by extrapolating the concentration form the signal equal to background plus 3 standard deviations. Error bars represent the standard deviations of three repetitions.

molecules. The PDMS femtoliter-sized array enables single-molecule detection straightforward using conventional optics cameras used in fluorescence microscopes. Using streptavidin and carboxyl coated magnetic beads, we demonstrated the capability of power-free arrays for performing digital bioassays. Moreover, the chip greatly simplified the process development, and the fabrication of this array is low-cost manufacturing and do not need complex surface modification. The experiments were accomplished using a conventional micropipette, and this provides a path towards the development of instrumentation for performing high-throughput testing of samples in single-molecule arrays for applications in life science research and in vitro diagnostics (Whitesides, 2006). Although our method has the ability to digitally detect biomolecules, the number of unique digital wells limits the dynamic range of detection. So further researches should be done to improve the upper limit and developing a new strategy to improve dynamic range for digital immunoassays is a must. More importantly, in the future, we will focus on the clinical applications of this method so that much more valuable information with practical implications can be found.

Declaration of interests

- The authors declare that they have no known competing financial interests or personal relationships that could have appeared to influence the work reported in this paper.
- The authors declare the following financial interests/personal relationships which may be considered as potential competing interests:

Conflict of interest

The authors declare no conflict of interest.

CRediT authorship contribution statement

Jingjing Sun: Conceptualization, Methodology, Visualization, Writing - original draft, Writing - review & editing. **Jiumei Hu:** Writing - review & editing. **Tong Gou:** Software, Writing - original draft. **Xiong Ding:** Writing - original draft. **Qi Song:** Conceptualization. **Wenshuai Wu:** Formal analysis. **Guoping Wang:** Formal analysis. **Juxin Yin:** Formal analysis. **Ying Mu:** Funding acquisition, Project administration.

Acknowledgments

The authors are grateful for the financial support from the National Key R&D Program of China (2018YFF01012100), the Fundamental Research Funds for the Central Universities (2-2050205-19-007) and the Autonomous Research Project of the State Key Laboratory of

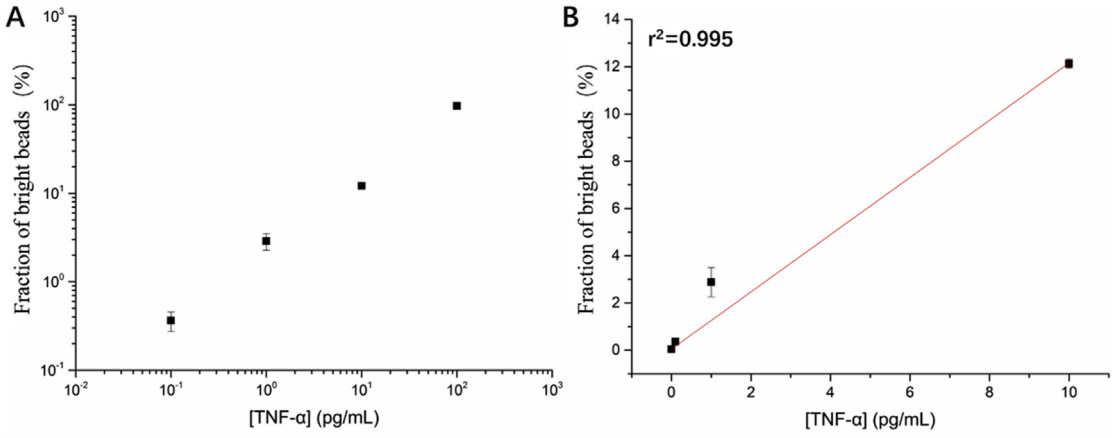

Fig. 6. Digital ELISA of TNF-α. (A) The plot shows the assay response over the concentration range tested in log-log space. (B) Expanded plot with linear-linear scale show the linearity of response. The limit of detection (12.62 fg/mL) was determined by extrapolating the concentration form the signal equal to background plus 3 standard deviations. Error bars represent the standard deviations of three repetitions.

Industrial Control Technology (No. ICT1805), Zhejiang University. China.

Appendix A. Supplementary data

Supplementary data to this article can be found online at https://doi.org/10.1016/j.bios.2019.111339.

References

Anderson, N.L., Polanski, M., Pieper, R., Gatlin, T., Tirumalai, R.S., Conrads, T.P., Veenstra, T.D., Adkins, J.N., Pounds, J.G., Fagan, R., Lobley, A., 2004. The human plasma proteome: a nonredundant list developed by combination of four separate sources. Mol. Cell. Proteom. 3 (4), 311–326.

Decrop, D., Pardon, G., Brancato, L., Kil, D., Zandi Shafagh, R., Kokalj, T., Haraldsson, T., Puers, R., van der Wijngaart, W., Lammertyn, J., 2017. Single-step imprinting of femtoliter microwell Arrays allows digital bioassays with attomolar limit of detection. ACS Appl. Mater. Interfaces 9 (12), 10418–10426.

Dong, J., Ueda, H., 2017. ELISA-type Assays of Trace Biomarkers Using Microfluidic Methods, vol. 9 Wiley Interdiscip Rev Nanomed Nanobiotechnol (5).

Giljohann, D.A., Mirkin, C.A., 2009. Drivers of biodiagnostic development. Nature 462 (7272), 461.

Hanash, S.M., Baik, C.S., Kallioniemi, O., 2011. Emerging molecular biomarkers–blood-based strategies to detect and monitor cancer. Nat. Rev. Clin. Oncol. 8 (3), 142–150.

Kan, C.W., Rivnak, A.J., Campbell, T.G., Piech, T., Rissin, D.M., Mosl, M., Peterca, A., Niederberger, H.P., Minnehan, K.A., Patel, P.P., Ferrell, E.P., Meyer, R.E., Chang, L., Wilson, D.H., Fournier, D.R., Duffy, D.C., 2012. Isolation and detection of single molecules on paramagnetic beads using sequential fluid flows in microfabricated polymer array assemblies. Lab Chip 12 (5), 977–985.

Kim, S.H., Iwai, S., Araki, S., Sakakihara, S., Iino, R., Noji, H., 2012. Large-scale femtoliter droplet array for digital counting of single biomolecules. Lab Chip 12 (23), 4986–4991.

Leirs, K., Tewari Kumar, P., Decrop, D., Perez-Ruiz, E., Leblebici, P., Van Kelst, B., Compernolle, G., Meeuws, H., Van Wesenbeeck, L., Lagatie, O., Stuyver, L., Gils, A., Lammertyn, J., Spasic, D., 2016. Bioassay development for ultrasensitive detection of influenza a nucleoprotein using digital ELISA. Anal. Chem. 88 (17), 8450–8458.

Liebherr, R.B., Hutterer, A., Mickert, M.J., Vogl, F.C., Beutner, A., Lechner, A., Hummel, H., Gorris, H.H., 2015. Three-in-one enzyme assay based on single molecule detection in femtoliter arrays. Anal. Bioanal. Chem. 407 (24), 7443–7452.

Rissin, D.M., Fournier, D.R., Piech, T., Kan, C.W., Campbell, T.G., Song, L., Chang, L., Rivnak, A.J., Patel, P.P., Provuncher, G.K., Ferrell, E.P., Howes, S.C., Pink, B.A., Minnehan, K.A., Wilson, D.H., Duffy, D.C., 2011. Simultaneous detection of single molecules and singulated ensembles of molecules enables immunoassays with broad dynamic range. Anal. Chem. 83 (6), 2279–2285.

Rissin, D.M., Kan, C.W., Campbell, T.G., Howes, S.C., Fournier, D.R., Song, L., Piech, T., Patel, P.P., Chang, L., Rivnak, A.J., Ferrell, E.P., Randall, J.D., Provuncher, G.K., Walt, D.R., Duffy, D.C., 2010. Single-molecule enzyme-linked immunosorbent assay detects serum proteins at subfemtomolar concentrations. Nat. Biotechnol. 28 (6), 595–599.

Rondelez, Y., Tresset, G., Tabata, K.V., Arata, H., Fujita, H., Takeuchi, S., Noji, H., 2005. Microfabricated arrays of femtoliter chambers allow single molecule enzymology. Nat. Biotechnol. 23 (3), 361–365.

Schubert, S.M., Walter, S.R., Manesse, M., Walt, D.R., 2016. Protein counting in single cancer cells. Anal. Chem. 88 (5), 2952–2957.

Shim, J.U., Ranasinghe, R.T., Smith, C.A., Ibrahim, S.M., Hollfelder, F., Huck, W.T., Klenerman, D., Abell, C., 2013. Ultrarapid generation of femtoliter microfluidic droplets for single-molecule-counting immunoassays. ACS Nano 7 (7), 5955–5964.

Song, L., Hanlon, D.W., Chang, L., Provuncher, G.K., Kan, C.W., Campbell, T.G., Fournier, D.R., Ferrell, E.P., Rivnak, A.J., Pink, B.A., Minnehan, K.A., Patel, P.P., Wilson, D.H., Till, M.A., Faubion, W.A., Duffy, D.C., 2011. Single molecule measurements of tumor necrosis factor alpha and interleukin-6 in the plasma of patients with Crohn's disease. J. Immunol. Methods 372 (1–2), 177–186.

Tekin, H.C., Gijs, M.A., 2013. Ultrasensitive protein detection: a case for microfluidic magnetic bead-based assays. Lab Chip 13 (24), 4711–4739.

Vogelstein, B., Kinzler, K.W., 1999. Digital PCR. Proc. Natl. Acad. Sci. U. S. A 96 (16), 9236–9241.

Walt, D.R., 2013. Optical methods for single molecule detection and analysis. Anal. Chem. 85 (3), 1258–1263.

Whitesides, G.M., 2006. The origins and the future of microfluidics. Nature 442 (7101), 368–373.

Wilson, D.H., Rissin, D.M., Kan, C.W., Fournier, D.R., Piech, T., Campbell, T.G., Meyer, R.E., Fishburn, M.W., Cabrera, C., Patel, P.P., Frew, E., Chen, Y., Chang, L., Ferrell, E.P., von Einem, V., McGuigan, W., Reinhardt, M., Sayer, H., Vielsack, C., Duffy, D.C., 2016. The Simoa HD-1 analyzer: a novel fully automated digital immunoassay analyzer with single-molecule sensitivity and multiplexing. J. Lab. Autom. 21 (4), 533–547.

Witters, D., Knez, K., Ceyssens, F., Puers, R., Lammertyn, J., 2013. Digital microfluidics-enabled single-molecule detection by printing and sealing single magnetic beads in femtoliter droplets. Lab Chip 13 (11), 2047–2054.

Wu, D., Katilius, E., Olivas, E., Dumont Milutinovic, M., Walt, D.R., 2016. Incorporation of slow off-rate modified aptamers reagents in single molecule array assays for cytokine detection with ultrahigh sensitivity. Anal. Chem. 88 (17), 8385–8389.

Zhang, H., Nie, S., Etson, C.M., Wang, R.M., Walt, D.R., 2012. Oil-sealed femtoliter fiber-optic arrays for single molecule analysis. Lab Chip 12 (12), 2229–2239.

Zhu, Q., Gao, Y., Yu, B., Ren, H., Qiu, L., Han, S., Jin, W., Jin, Q., Mu, Y., 2012. Self-priming compartmentalization digital LAMP for point-of-care. Lab Chip 12 (22), 4755–4763.